Bulletin of the Chemists and Technologists
Glasnik hemičara i tehnologa Bosne i Hercegovine
2026
66
13-21
Original Scientific Article
Print ISSN: 0367-4444
Online ISSN: 2232-7266
DOI: 10.35666/2232-7266.2026.66.02
UDK: 543[547.79:547.78]

Understanding MTT–Graphene Oxide Interactions for Accurate Viability Measurements

Ćetković Pećar, T.[a], Haverić, A.[a], Haverić, S.[a], Gutić, S.J.[b,*]

[a]*University of Sarajevo – Institute for Genetic Engineering and Biotechnology, Zmaja od Bosne 8, Sarajevo, Bosnia and Herzegovina*

[b] *University of Sarajevo – Faculty of Science, Zmaja od Bosne 33-35, Sarajevo, Bosnia and Herzegovina*

Article info
Received: 03/12/2025
Accepted: 04/02/2026

Keywords:
Colorimetric assay
MTT assay
Graphene oxide
Adsorption
Nanomaterial interference

***Corresponding author:**
E-mail: sgutic@pmf.unsa.ba
Phone: +-387-61-337636

Abstract: Large surface enriched with oxygen-containing groups, enabling interactions with various molecules, makes graphene oxide (GO) valuable in sensing, imaging, and therapy but complicates cytotoxicity assessment using standard colorimetric assays. In this study we examined adsorption of tetrazolium (MTT) ion, used as a dye in colorimetric assay, on GO. Using a cell-free system, adsorption behavior was modelled with Freundlich, Langmuir, and Langmuir–Freundlich (Sips) isotherms. Satisfactory fits were obtained by all models. However, the Sips model provided the best nonlinear regression performance, while Langmuir fit best under linear regression. π–π interactions between MTT and the GO aromatic rings were discussed as the most probable driving force for the adsorption. Interactions between GO and components of the culture medium (DMEM) and serum (FBS) were indirectly observed by comparing MTT monolayer capacity values with the values obtained in aqueous MTT solutions. The results confirm that GO interactions with MTT, responsible for the interferences, can be described quantitatively in the presence of cell supporting medium and that corrective adjustments of the colorimetric assay results may be required, yet the question remains whether such corrections can be applied in practice. The present study provides an initial foundation for assessing their feasibility.

INTRODUCTION

Growing interest for the application of graphene nanomaterials (GNMs) in the biotechnological and biomedical fields has been evident (Kumar et al., 2023). Accordingly, accurate *in vitro* assessment of their potential cytotoxicity, oxidative stress induction, genotoxicity, and inflammatory effects, along with determination of the mechanisms of action of GNMs in cell membrane and cellular components damage is crucial (Gurunathan S et al., 2019; Frontiñan-Rubio et al., 2022).

Classical methods for cytotoxicity investigation are based on colorimetric tests with organic tetrazolium dyes, such as 3-(4,5-di methyl thiazol-2-yl)-2,5-diphenyltetrazolium bromide (MTT) (van Meerloo et al., 2011). Despite the large number of studies reporting the use of the MTT assay for the toxicological evaluation of graphene oxide nanomaterials (Seabra et al., 2014), several have also highlighted specific limitations that may affect the accuracy and reliability of cytotoxicity assessments of namely carbon-nanotubes (Wörle-Knirsch et al. 2006; Casey et al. 2007a, Ali-Boucetta et al., 2011), graphene (Jiao et al., 2015) and graphene oxide (Liao et al., 2011). Challenges in cytotoxicity assessment of nanoparticles in general are related to diverse potential interactions between nanoparticles and dye molecules, or their reduced forms (formazans), and those interactions can be very specific (Jiao et al., 2015; Monteiro-Riviere et al., 2009; Belyanskaya et al., 2007; Wörle-Knirsch et al., 2006). The study by Wörle-Knirsch et al. (2006) demonstrated that single-walled carbon nanotubes (SWCNTs) interact with MTT formazan crystals, leading to inaccurate assay results. Additionally, Casey et al. (2007a) showed that dispersing (SWCNTs) in cell culture medium induces color changes due to molecular interactions with medium components, as confirmed by spectroscopic analysis. Moreover, they demonstrated that SWCNTs interfered with several viability assays, including MTT, by interacting with indicator dyes and reducing their absorbance in a concentration-dependent manner (Casey et al., 2007b).

Under the "graphene" umbrella one can find various materials (eg. graphene oxide, reduced graphene oxide, quantum dots, etc.) with a variety of physical and chemical features including specific shape and size, crystalline structure and presence of various functional groups and structural defects, which makes generalization of their impact on the reliability of cytotoxicity assessment practically impossible.

Graphene oxide (GO) nanomaterials possess the ability to adsorb biomolecules via multiple interaction mechanisms, including hydrogen bonding, hydrophobic interactions, π-π stacking, and both electrostatic and van der Waals forces (Nel et al., 2009). Such interactions facilitate the adsorption of proteins from fetal bovine serum onto the GO surface, leading to the formation of a protein corona that further alters the nanomaterial's physicochemical properties and biological interactions (Cedervall et al., 2007; Hu et al., 2011; Wei et al., 2015). Optical characteristics of graphene can present additional challenges for *in vitro* tests, particularly due to absorption and reflection effects. Some studies have shown that absorption increases with the thickness of the graphene layer, with each additional graphene layer contributing to a 2.3% rise in absorption intensity (Nair et al., 2008; Bonaccorso et al., 2010). As a result, the optical properties of graphene may lead to the loss of light signals during *in vitro* studies (Jiao et al., 2015).

In this work we investigated interactions of MTT with commercially available GO material in simple aqueous solutions as well as in the presence of Dulbecco's Modified Eagle Medium (DMEM) and Fetal Bovine Serum (FBS). Experimentally obtained adsorption data was modelled with Freundlich, Langmuir, and Langmuir-Freundlich isotherms by both linear and nonlinear regression. Specific interactions between MTT and GO, as well as the differences in the values of adsorption constants for simple aqueous solutions and solutions containing cell supporting medium were discussed in accordance with structural features obtained from the detailed GO characterization.

Perspective was given on the feasibility of the introduction of experimental correction in the MTT assay, based on the knowledge on the adsorption behavior.

EXPERIMENTAL

Materials and chemicals

All materials used in this study, including commercially available graphene oxide (4 mg mL^{-1} suspension)[1], Dulbecco's Modified Eagle Medium (DMEM), fetal bovine serum (FBS), and the MTT reagent, were obtained from Sigma-Aldrich (St. Louis, MO, USA).

Material characterization

Graphene oxide was characterized by Fourier transform infrared spectroscopy (FTIR), Raman spectroscopy, X-ray diffraction (XRD), and cyclic voltammetry (CV).

Fourier-transform infrared (FTIR) spectra were recorded in attenuated total reflectance (ATR) mode using a PerkinElmer UATR Two spectrometer. Aqueous suspensions were drop-casted directly onto the ATR crystal and dried at room temperature. Spectra were collected at room temperature over the range of 400 to 4000 cm^{-1}, with a resolution of 1 cm^{-1}.

Raman spectra were obtained with a DXR Raman microscope (Thermo Scientific, USA) equipped with an Olympus optical microscope and a CCD detector. The sample was prepared by drop-casting of aqueous suspension onto a gold surface. Raman spectra were collected for dry GO sample, by excitation with a HeNe gas laser (excitation wavelength 532 nm) beam focused using magnification 50×. The scattered photons were analyzed by the spectrograph with a grating of 900 lines mm^{-1}. Laser power on the sample was kept at 2 mW.

X-ray diffraction (XRD) patterns were collected for the sample suspended in water, using a Bruker D8 Advance diffractometer with Cu Kα1,2 radiation source. Generator voltage and current were 40.0 kV and 40.0 mA, respectively.

Cyclic voltammetry was performed using a three-electrode setup with Ag/AgCl/KClsat as the reference and a platinum wire as the counter electrode. Working electrode was prepared by drop-casting 10 μL of sample suspension (1 mg mL^{-1}) onto a clean glassy carbon disc (d = 5 mm). Measurements were conducted in 0.1 M KNO_3 over the reduction potential range (from open circuit to hydrogen evolution onset) at a sweep rate of 15 mV s^{-1}.

Spectrophotometric measurements

To investigate interactions of the graphene oxides with the MTT dye, each GO was incubated with a series of MTT dilutions in cell-free systems (Jiao et al., 2015), using two different adsorption media: (i) deionized water, denoted as W; (ii) deionized water with Dulbecco's Modified Eagle Medium (DMEM) supplemented with fetal bovine serum (FBS), denoted as WMS. In both cases MTT concentrations were 0.01, 0.02, 0.05, 0.07, 0.1, and 0.2 mg mL^{-1}. Each dilution contained 1 mg (0.44 mg mL^{-1}) of graphene oxide. Calibration curve was recorded by measuring the aqueous solutions of MTT without graphene oxide. All adsorption series were corrected with the corresponding blank – deionized water for W, and deionized water with DMEM and FBS for WMS samples. After 24 hours of incubation at 37°C with continuous mixing, a series of MTT reagent dilutions were added to each mixture, followed by an additional 3-hour incubation under the same conditions. Following MTT incubation, all samples were centrifuged at 16000 rpm for 10 minutes. Clear supernatants were transferred to 96 well plate in duplicate, and their absorbance was measured at 380 nm with the ThermoFisher Scientific Multiskan SkyHigh Microplate Spectrophotometer.

[1] https://www.sigmaaldrich.com/BA/en/product/aldrich/777676?context=product

RESULTS AND DISCUSSION

Characterization of graphene oxide

Typical absorption peaks expected for graphene oxides prepared by Hummers method can be observed in the infrared spectra of GO (Fig. 1). Adsorbed water molecules are responsible for the strong overlapping absorptions in the region between 2400 and 3700 cm^{-1}, as well as at 1620 cm^{-1} (Brusko et al., 2024). Although not observed for highly oxidized graphene oxides, peak at 1585 cm^{-1} is clearly observed for the GO sample. This absorption is connected to C=C stretching in the graphene lattice, and usually appears for partially reduced graphene oxides. Absorption at 1725 cm^{-1} is typical spectral feature of graphene oxide, originating from stretching of C=O bond from carboxylic groups, as well as any other carbonyl groups (Eigler and Dimiev, 2017) while shoulder at 1815 cm^{-1} probably originates of the C=O bond stretch in the ketone group. The band with the highest intensity in the fingerprint region of the spectra, observed at 1073 cm^{-1}, arise probably from the C-O vibrations in alcohol functional groups. Other two prominent bands from the fingerprint region, at 1411 and 1233 cm^{-1}, originate from covalently attached sulfate groups, which are present due to the preparation method (Brusko et al., 2024), although the latter can also be connected to epoxy groups (C-O-C), vibrations of which are responsible for the shoulder at 980 cm^{-1}.

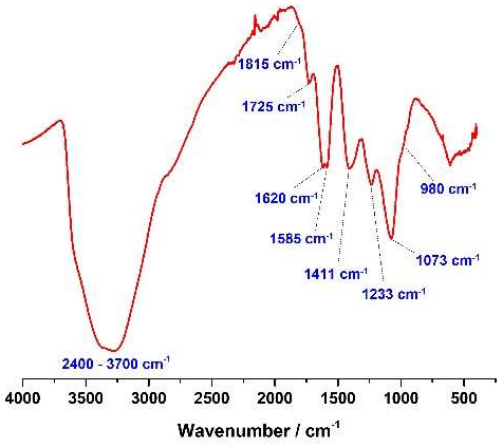

Figure 1. ATR-FTIR spectrum of dry graphene oxide

First and second order Raman spectra of dry GO sample, shown in Figure 2, were deconvoluted and with several characteristic peaks, as shown in Figure 2 (b. and c.). Although five peaks were used to fit the first-order spectrum of the sample, only four of them, namely D, D'', G, and D' have physical significance (López-Díaz et al., 2020). The shoulder arising from the D* peak, usually positioned around 1150 cm^{-1}, was not observed for this GO sample. Position of the nondispersive G peak was red-shifted to 1573 cm^{-1} (from 1585 cm^{-1} usually observed for graphene oxide), which may be an indication of AB stacking of graphene layers. The peaks arising from structural and chemical defects, denoted by D' and D, appear at 1610 cm^{-1} and 1355 cm^{-1}, respectively. Intensity ratio of these peaks, $A_{D'}/A_D$, can be used for the estimation of the dominant type of defects. In our case $A_{D'}/A_D$ was 0.082, indicating prevalence of sp^3 defects, caused by sulfate and oxygen-containing functional groups covalently attached to graphene basal plane. Position of another peak from the deconvoluted first-order spectrum, designated as D" and observed at 1500 cm^{-1}, reveals that oxygen content should be below 20 at% (Lopez-Díaz et al., 2017; Claramunt et al., 2015). Second-order part of the spectra was fitted with four Gaussian peaks designated as G*, 2D, D+D', and 2D'. Positions of the 2D and D+D' bands can be used for the estimation of percentage of sp^2-hybridized C atoms in graphene. For the GO sample wide 2D band appears at 2736 cm^{-1}, while D+D' band appears at 2932 cm^{-1}. FWHM value of 149 cm^{-1} for the former (six-fold the value for the pristine graphene) indicates that "2D" peak in fact consists of several overlapping peaks, which are not studied in detail in this work, thus position of wide "2D" peak cannot be used for the same estimation. However, position of the D+D' corresponds to the 51.7 % of sp^2 carbon atoms (López-Díaz et al., 2020), compared with the 63.1 %, estimated from the I_D/I_G ratio of 1.505 (Lopez-Díaz et al., 2017).

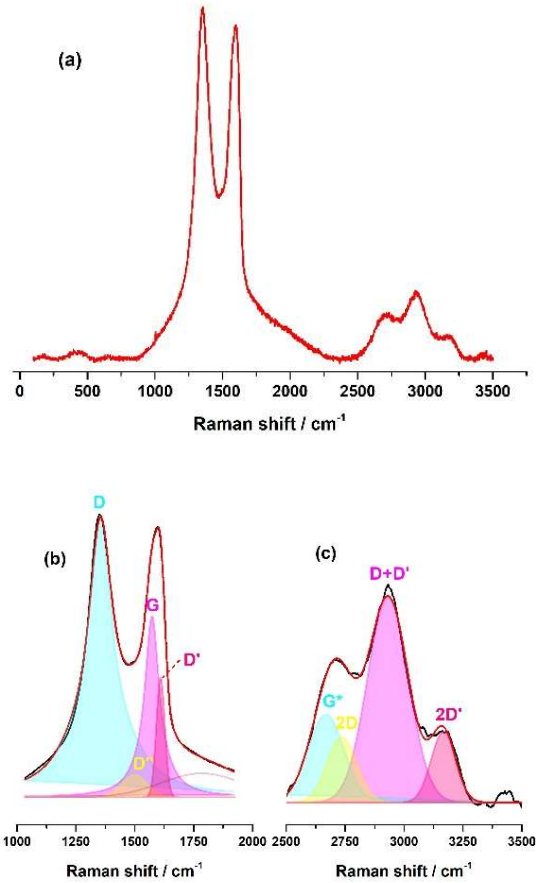

Figure 2. (a) Raman spectrum of dry graphene oxide; (b) First order Raman peaks; (c) second order Raman peaks.

XRD pattern of the GO sample (Figure 3) reveals weak and diffuse (002) graphite reflection around $2\theta = 25°$, while the characteristic graphene-oxide reflection at 2θ = 11.8°, arising from the larger distance between graphene-oxide

sheets (around 8 Å) compared to those of graphite, is not observed. Absence of this characteristic diffraction indicates high level of graphitization, which is in accordance with some features observed in Raman spectrum.

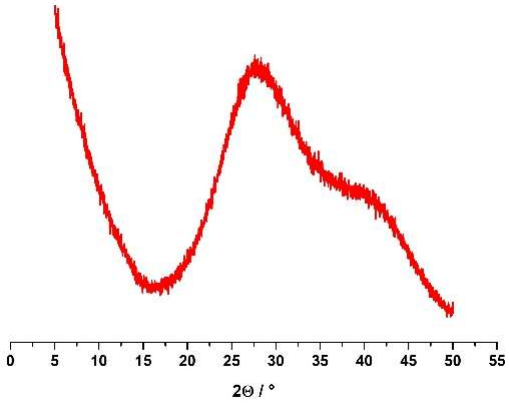

Figure 3. X-ray diffraction pattern of suspended graphene oxide

Redox behavior, estimated by cyclic voltammetry (Figure 4), is in accordance with the structural features observed from FTIR and Raman spectroscopies. First potential scan in negative direction leads to typical cathodic current peak at -1.4 V vs. Ag/AgCl reference, arising from the irreversible GO reduction, evident from the absence of corresponding oxidation peak on the backward scan, as well as the absence of reduction/oxidation peaks in the second scan. Specific charge consumed for the reduction of GO is 4.2 mC μg^{-1}, which gives a rough estimation of 52 % of sp^3 carbons with covalently attached reducible functional groups.

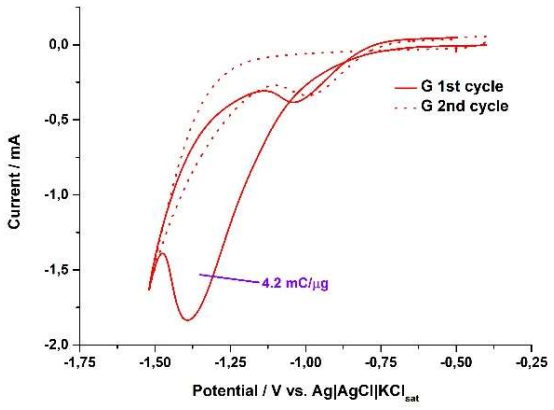

Figure 4. Cyclic voltammograms of graphene oxide film reduction in inert electrolyte

Adsorption of MTT

Nanomaterials introduced into complex culture media, especially those supplemented with FBS, undergo various physicochemical interactions that can significantly alter their surface properties and biological behavior. In particular, the rapid formation of a protein corona modifies their biological identity, affecting interactions with cells, medium components, and assay outcomes, as pointed in the literature (Cedervall et al., 2007; Hu et al., 2011; Wei et al., 2015). To try to elucidate the contribution of different components present during the colorimetric testing of viability, adsorption behavior of MTT dye was determined from two different adsorption media: (i) aqueous MTT solutions without additional components (denoted as "W"), and (ii) aqueous solutions containing constant concentration of Dulbecco's Modified Eagle Medium (DMEM) and Fetal Bovine Serum (FBS) (denoted as "WMS").

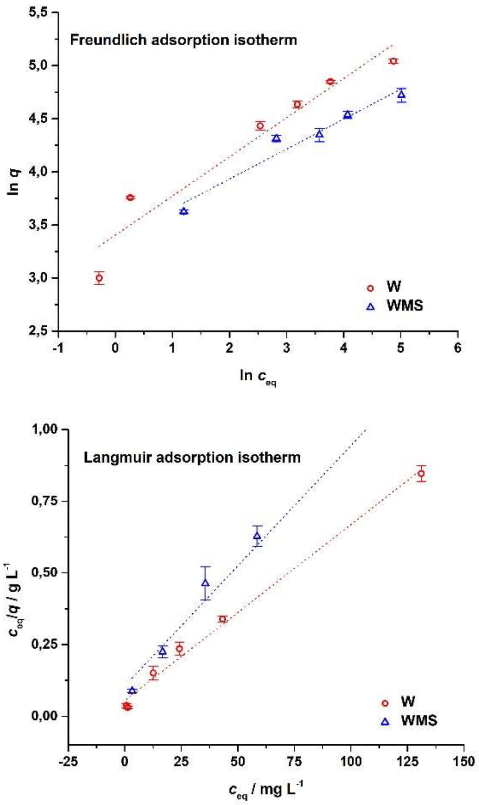

Figure 5. Adsorption of MTT on graphene oxide: linear fits of experimental results with Freundlich and Langmuir isotherm.

Three adsorption isotherms were used for fitting of the experimentally obtained results:

(i) Freundlich adsorption isotherm

$$q = k_F c_{eq}^{1/n} \quad (1)$$

(ii) Langmuir adsorption isotherm

$$q = \frac{q_{max} K_L c_{eq}}{1 + K_L c_{eq}} \quad (2)$$

(iii) Langmuir-Freundlich (Sips) adsorption isotherm

$$q = \frac{K_{LF} c_{eq}^{b_{LF}}}{1 + a_{LF} c_{eq}^{b_{LF}}} \quad (3)$$

where q / mg g^{-1} is the mass of the adsorbed MTT per unit mass of the adsorbent, c_{eq} / mg L^{-1} equilibrium concentration of MTT, and k_F, n, K_L, q_m, K_{LF}, a_{LF}, and b_{LF} constants for a particular isotherm. Data fitting was

performed by two approaches: (i) in MS Excel, using linear forms of Freundlich and Langmuir isotherms, and (ii) in online Desmos Graphing Calculator (https://www.desmos.com/), by nonlinear regressions for all three isotherms.

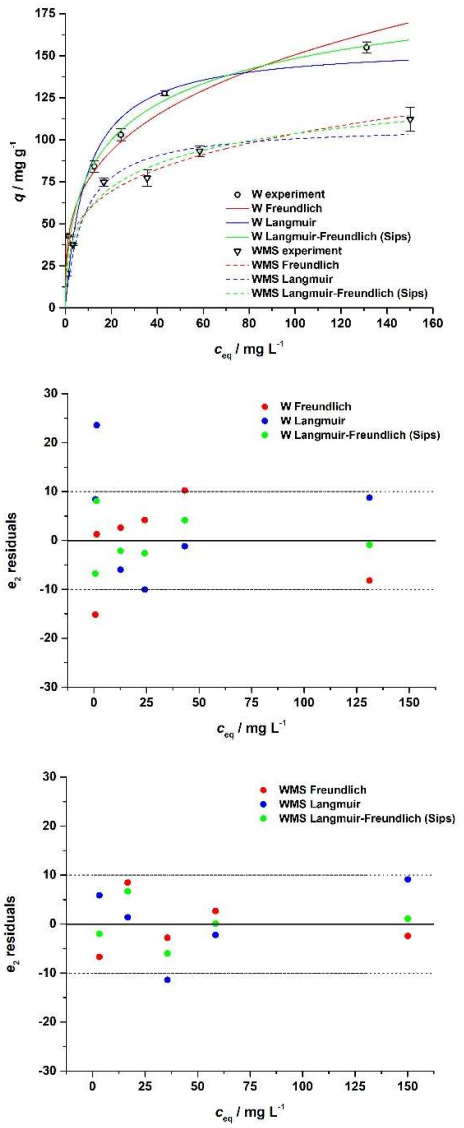

Figure 6. Nonlinear fits of experimental results with Freundlich, Langmuir and Langmuir-Freundlich (Sips) isotherms with corresponding e_2 residuals

Correlation coefficients for linear fitting of the experimental results have higher values when Langmuir model is applied, compared to the values obtained from the Freundlich model, for both adsorption media (Table 1, Figure 5). However, in nonlinear approach (Table 1, Figure 6) the correlation coefficients decrease in the order Langmuir-Freundlich (Sips) > Freundlich > Langmuir for both adsorption media. Comparing the linear and nonlinear regression for Freundlich and Langmuir models reveals that nonlinear approach leads to a better fit for Freundlich model, while linear approach gives better correlation for Langmuir model. It is also important to note that in the case of Freundlich model nonlinear fit leads to higher values of constants, compared to the linear fit, while the opposite is true for Langmuir model. Differences between parameter values obtained by linear and nonlinear regression arise from distortions in the error distribution caused by data transformation during linearization (Hu et al., 2023). Although linearization is straightforward and commonly used, isotherm parameters derived in this manner are presented here only to highlight the bias introduced by linearization. In the following discussion parameters obtained from nonlinear regression will be considered, particularly because of the application of the multi-parameter Langmuir–Freundlich (Sips) model.

Table 1: Adsorption isotherm parameters

Freundlich adsorption isotherm

Medium	W		WMS	
Fitting	Linear	Nonlinear	Linear	Nonlinear
k_F [*1]	30±2	38±1	29±1	32.9±0.1
n	2.7±0.1	3.4±0.1	3.6±0.3	4.0±0.2
R^2	0.9346	0.9670	0.9500	0.9550

Langmuir adsorption isotherm

Medium	W		WMS	
Fitting	Linear	Nonlinear	Linear	Nonlinear
K_L [*2]	0.11±0.02	0.109±0.007	0.079±0.005	0.13±0.02
q_{max} [*3]	163±4	156±1	120±8	109±9
R^2	0.9927	0.9350	0.9922	0.9169

Langmuir-Freundlich (Sips) adsorption isotherm

Medium	W		WMS	
Fitting	Linear	Nonlinear	Linear	Nonlinear
K_{LF} [*4]	-	36±2	-	29±3
a_{LF} [*5]	-	0.15±0.01	-	0.18±0.02
b_{LF}	-	0.531±0.008	-	0.50±0.06
R^2	-	0.9891	-	0.9718

[*1] / (mg/g)/(L/mg)^n; [*2] / L/mg; [*3] / mg/g; [*4] / L/g; [*5] / L/mg

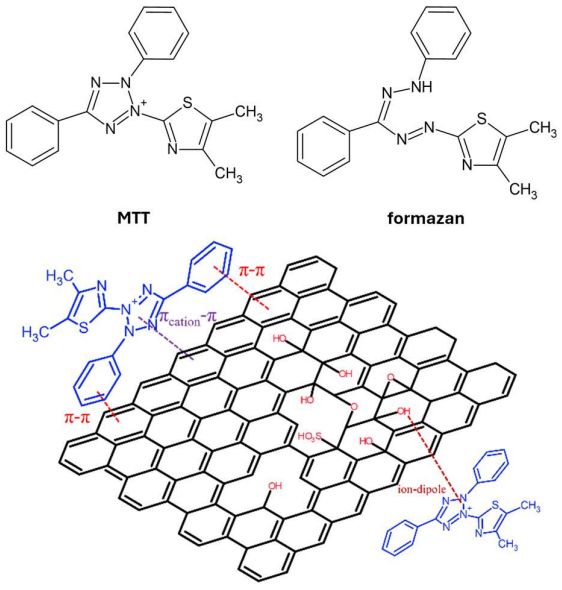

Figure 7. Structures of MTT, formazan and graphene oxides, and some of the possible interactions between the MTT molecule and graphene oxide.

Characterization of the sample, as discussed earlier, revealed some basic features of the graphene oxide structure, which are responsible for interactions with MTT dye, as well as with other components of the medium. Between 50 and 60 % of the carbon atoms from the GO sample structure are sp^3-hybridized and covalently connected to polar functional groups such as alcohol, epoxy, carbonyl or sulfate, that enable interaction with the adsorbate species via dipole-dipole or dipole-ion interactions. The difference between the percentage of sp^3-hybridized C atoms and the estimated oxygen content (less than 20 %) is potentially related to the high content of epoxy groups, compared to other functionalities. In any case, the rest of the C atoms (40 – 50 % of sp^2-hybridized) form aromatic graphene structure which enables π-π interactions with the species containing aromatic rings.

Both MTT and the corresponding formazan molecule (Fig. 7), contain aromatic rings that can interact with the graphene via π-π interactions (Fig. 7). Furthermore, MTT dye is aromatic cation available and applied in a form of bromide salt, which opens up the possibility for a different types of interactions, including π_{cation}-π, dipole-ion or even ionic interactions with anionic groups on graphene at the higher pH values (Fig. 7). Interaction energies drop several orders of magnitude in the series ion-ion > dipole-ion > π_{cation}-π > π-π (Georgakilas et al., 2012), implying that the former will be thermodynamically favorable. However, the positive charge of the MTT ion is located in the aromatic ring, with the two exposed benzene rings, which significantly increases contribution of π_{cation}-π and π-π interactions in bulk adsorption (Georgakilas et al., 2012). Furthermore, in aqueous solution dominant functional groups attached to the graphene surface are either unable to dissociate (epoxy groups) or are very weak acids (alcohol groups) (Lu et al., 2021), which leaves a small fraction of acidic groups (sulfate and carboxylic) for the ion-ion interaction. Variety of the possible interactions is in the agreement with the values of the constants n and b_{LF} (Table 1.) obtained from fitting with Freundlich and Langmuir-Frenudlich (Sips) model respectively, which point to the heterogeneous adsorption (Murphy et al., 2023).

The MTT assay is based on a spectrophotometric measurement of formazan, a colored product formed through the reduction of the yellow, water-soluble tetrazolium salt (MTT) by mitochondrial dehydrogenases, cytoplasmic NAD(P)H-dependent oxidoreductases and other reducing agents in metabolically active cells. The reduction of MTT yields a violet-blue, water-insoluble formazan that accumulates in lipid droplets and can be solubilized with organic solvents for spectrophotometric quantification of cell viability. It is important to note that adsorption studies performed in cell-free systems capture only part of the complexity of cytotoxicity assays. While they provide valuable information on physicochemical interactions between graphene nanomaterials and assay components (Monteiro-Riviere et al., 2009), real cellular environments introduce additional layers of complexity, including membrane dynamics, metabolic activity, intracellular trafficking, and signaling cascades. These processes can modulate both the extent and the biological consequences of adsorption, meaning that results obtained in simplified systems should be interpreted as complementary to cellular assays. This distinction is crucial for accurate evaluation of the biological impact of graphene nanomaterials.

Since the reduction product (formazan) is the species quantified in the assay, it is necessary to consider whether adsorption of its precursor (MTT) alone is sufficient to evaluate the impact of interactions with the material studied on assay outcomes. Given that the graphene oxide particles used here have size distributions of D90 = 5–7 µm, D50 = 2–4 µm, and D10 = 1–2 µm (https://www.sigmaaldrich.com/BA/en/product/aldrich/777676?srsltid=AfmBOopH5rtQ6uspqC8TFsQ_1N6ru6UvIOYDsiFd66a1hsFRCe733lUg, accessed 29/12/2025), comparable to the size of cells typically analyzed by the MTT assay, internalization of GO particles carrying adsorbed MTT is limited, thereby preventing intracellular formazan formation. Consequently, measurements of MTT adsorption are sufficient for assessing assay interference in cytotoxicity studies involving cells of comparable dimensions. Under these conditions, measurements of MTT adsorption may provide a reasonable approximation for evaluating assay interference in cytotoxicity studies involving cells of comparable dimensions.

Based on its molecular structure, we hypothesize that the corresponding formazan may also interact with graphene oxide, predominantly through π–π interactions, as it is an electrically neutral molecule with weak dipole moments. This raises the possibility that, even if MTT–GO complexes are internalized and MTT is subsequently reduced within viable cells, the resulting formazan may remain susceptible to adsorption onto graphene oxide. Such interactions could reduce the fraction of free formazan available for optical detection, thereby potentially compromising the reliability of absorbance-based cytotoxicity measurements.

Adsorption of proteins and other components of the fetal bovine serum, described in the literature (Cedervall et al., 2007; Hu et al., 2011; Wei et al., 2015), is evident from the decrease in the Langmuir's monolayer adsorption capacity, q_{max}. For the adsorption of MTT from pure aqueous solution q_{max} has a value of 156 mg g^{-1}, while the same parameter dropped to 109 mg g^{-1} for the adsorption of MTT from a solution containing DMEM and FBS. Influence of DMEM and FBS on the adsorption strength of MTT is also observable from the lower Freundlich constant (k_F) values, compared to values obtained from the simple aqueous solution of MTT, indicating weaker MTT-GO interactions when other adsorbates are present. DMEM and FBS components – soluble proteins and salts – compete with the MTT molecules for the hydrophilic and ionic adsorption sites, leaving aromatic sites for the exclusive adsorption of MTT through weaker π-π interactions. Another noteworthy observation is that values of a_{LF} and b_{LF} did not differ significantly for simple aqueous solutions and solutions containing DMEM and FBS, while the K_{LF} value reduced from 36 to 29 L g^{-1}. Since ratio K_{LF}/a_{LF} represents the monolayer adsorption capacity (Wang and Guo, 2020) obtained from Langmuir-Freundlich model values of 240 and 161 mg g^{-1} were calculated for adsorption of MTT from simple aqueous solution and solution with DMEM and FBS, respectively. As in the case for the q_{max} values determined from

Langmuir model, monolayer capacity for MTT is higher in aqueous solution without DMEM and FBS. However, Langmuir isotherm describes homogenous monolayer adsorption, while Langmuir-Freundlich (Sips) model assumes several different absorption sites with distinct adsorption energies, which makes the latter more relevant for quantitative description when graphene oxide acts as adsorbent for MTT. Although the Freundlich adsorption isotherm is one of the most widely used empirical models, while Langmuir adsorption isotherm is the most famous theoretical model, neither model alone adequately describes the heterogeneous nature of the present system, involving both the adsorbent (graphene oxide) and the adsorbates (MTT and other medium components) over a wide concentration range. While Freundlich isotherm provides satisfactory fits over medium concentration ranges and does not predict a saturation plateau at high concentrations, the applicability of the Langmuir isotherm is restricted to the adsorption of non-interacting adsorbate molecules on energetically equivalent sites (Hu et al., 2023; Al-Ghouti and Da'ana 2020). These limitations are evident from the residuals obtained by nonlinear fitting (Fig. 6). In contrast, satisfactory fits across the entire concentration range are achieved using the Sips adsorption isotherm, which combines features of the Langmuir and Freundlich models.

CONCLUSIONS

The results suggest that the affinity between graphene oxide and MTT arises from multiple possible interaction mechanisms, including π–π, dipole–dipole, and limited dipole–ion interactions. Structural characterization indicates that both sp^2-hybridized aromatic domains and oxygen-containing functional groups bonded to sp^3 carbon atoms contribute to these interactions, which aligns with isotherm parameters indicating a heterogeneous adsorption environment. The exposed aromatic rings of MTT favour π–π interactions with aromatic graphene regions, while the sterically shielded ionic center limits stronger ion–ion and ion-dipol contributions. According to these considerations the corresponding formazan product is also expected to adsorb strongly and remain non-desorbed under assay conditions.

Quantitative modelling further supports these mechanistic insights. Although linear regression suggests better performance of the Langmuir model, nonlinear fitting reveals that the Langmuir–Freundlich (Sips) model most accurately describes the adsorption behaviour, reflecting the heterogeneity of GO surface sites. The competition between MTT and supporting medium components is evident from reduced adsorption parameters in DMEM/FBS-containing solutions, indicating that proteins and salts occupy hydrophilic or ionic adsorption sites while leaving aromatic π-domains available for weaker interactions with MTT. This effect is consistently reflected in decreases in both Langmuir monolayer capacity and Langmuir–Freundlich model parameters.

Taken together, these findings provide a description of graphene oxide interactions with MTT under conditions relevant to cytotoxicity testing. The results quantitatively demonstrate that medium constituents significantly modulate adsorption behaviour and that both MTT and formazan can remain bound to GO with limited desorption. These mechanistic and modelling insights form a necessary foundation for evaluating how such interactions affect spectrophotometric readouts and represent an important first step toward assessing the broader implications for the reliability of colorimetric cell viability assays involving graphene-based nanomaterials.

Since the graphene oxide used in this study represents a highly specific material within the graphene family, the findings presented here cannot be directly extrapolated to other materials, even within the "graphene oxide" subcategory. To generalize the impact of graphene oxide on the reliability of cytotoxicity assessments, further studies employing multiple, thoroughly characterized GO materials are required. In contrast, generalization of the behavior across the entire graphene family appears impractical due to the extensive diversity of structural and chemical characteristics. Also, further investigation of formazan adsorption to graphene oxide is essential to clarify its contribution to assay interference and to improve the reliability of absorbance-based cytotoxicity assessments involving graphene-derived materials.

REFERENCES

Al-Ghouti, M. A., Da'ana, D. A. (2020). Guidelines for the use and interpretation of adsorption isotherm models: A review. *Journal of Hazardous Materials*, 393, 122383.

Ali Boucetta, H., Al Jamal, K. T., Müller, K. H., Li, S., Porter, A. E., Eddaoudi, A., Prato, M., Bianco, A., & Kostarelos, K. (2011). Cellular uptake and cytotoxic impact of chemically functionalized and polymer coated carbon nanotubes. *Small*, 7(22), 3230–3238.

Belyanskaya, L., Manser, P., Spohn, P., Bruinink, A., & Wick, P. (2007). The reliability and limits of the MTT reduction assay for carbon nanotubes–cell interaction. *Carbon*, 45(13), 2643–2648.

Bonaccorso, F., Sun, Z., Hasan, T., & Ferrari, A. C. (2010). Graphene photonics and optoelectronics. *Nature Photonics, 4*(9), 611–622.

Brusko, V., Khannanov, A., Rakhmatullin, A., Dimiev, A. M. (2024). Unraveling the infrared spectrum of graphene oxide. *Carbon*, 229.

Casey, A., Davoren, M., Herzog, E., Lyng, F. M., Byrne, H. J., & Chambers, G. (2007a). Probing the interaction of single-walled carbon nanotubes within cell culture medium as a precursor to toxicity testing. Carbon, 45, 34–40.

Casey, A., Herzog, E., Davoren, M., Lyng, F. M., Byrne, H. J., & Chambers, G. (2007b). Spectroscopic analysis confirms the interactions between single walled carbon nanotubes and various dyes commonly used to assess cytotoxicity. *Carbon*, 45, 1425–1432.

Cedervall, T., Lynch, I., Lindman, S., Berggård, T., Thulin, E., Nilsson, H., … & Linse, S. (2007). Understanding the nanoparticle–protein corona using methods to quantify exchange rates and affinities of proteins for nanoparticles. *Proceedings of the National Academy of Sciences*, 104(7), 2050–2055.

Claramunt, S., Varea, A., Lopez-Díaz, D., Velázquez, M. M., Cornet, A., Cirera, A. (2015). The importance of interbands on the interpretation of the Raman spectrum of graphene oxide. *The Journal of Physical Chemistry C*, 119, 10123–10129.

Eigler, S., Dimiev, A. M. (2017). Characterization techniques. In A. M. Dimiev & S. Eigler (Eds.), *Graphene oxide: Fundamentals and applications* (pp. 85–120). John Wiley & Sons.

Frontiñan Rubio, J., González, V. J., Vázquez, E., & Durán Prado, M. (2022). Rapid and efficient testing of the toxicity of graphene related materials in primary human lung cells. *Scientific Reports*, 12(1), 7664.

Geograkilas, V., Otyepka, M., Bourlinos, A. B., Chandra, V., Kim, N., Kemp, K. C., Hobza, P., Zboril, R., Kim, K. S., (2012). Functionalization of Graphene: Covalent and Non-Covalent Approaches, Derivatives and Applications. *Chemical Reviews*, 112, 6156–6214.

Gurunathan, S., Arsalan Iqbal, M., Qasim, M., Park, C. H., Yoo, H., Hwang, J. H., … & Hong, K. (2019). Evaluation of graphene oxide induced cellular toxicity and transcriptome analysis in human embryonic kidney cells. *Nanomaterials*, 9(7), 969.

Hu, W., Peng, C., Lv, M., Li, X., Zhang, Y., Chen, N., Fan, C., & Huang, Q. (2011). Protein corona-mediated mitigation of cytotoxicity of graphene oxide. *ACS Nano*, 5(5), 3693–3700.

Hu, Q., Lan, R., He, L., Liu, H., Pei, X. (2023). A critical review of adsorption isotherm models for aqueous contaminants: Curve characteristics, site energy distribution and common controversies. *Journal of Environmental Management*, 329, 117104

Jiao, G., He, X., Li, X., Qiu, J., Xu, H., Zhang, N., & Liu, S. (2015). Limitations of MTT and CCK-8 assay for evaluation of graphene cytotoxicity. *RSC Advances*, 5(66), 53240–53244.

Kumar, R., Singh, D. P., Muñoz, R., Amami, M., Singh, R. K., Singh, S., & Kumar, V. (2023). Graphene based materials for biotechnological and biomedical applications: Drug delivery, bioimaging and biosensing. Materials Today Chemistry, 33, 101750.

Liao, K. H., Lin, Y. S., Macosko, C. W., & Haynes, C. L. (2011). Cytotoxicity of graphene oxide and graphene in human erythrocytes and skin fibroblasts. *ACS Applied Materials & Interfaces*, 3, 2607–2615.

López-Díaz, D., Delgado-Notario, J. A., Clericò, V., Diez, E., Merchán, M. D., Velázquez, M. M. (2020). Towards understanding the Raman spectrum of graphene oxide: The effect of the chemical composition. *Coatings*, 10(6), 524.

Lopez-Díaz, D., Lopez Holgado, M., García-Fierro, J. L., Velázquez, M. M. (2017). Evolution of the Raman spectrum with the chemical composition of graphene oxide. *The Journal of Physical Chemistry C*, 121, 20489–20497.

Lu, Y., Huang, L., Guo, Y., Yang, X. (2021). Theoretical insights into origin of graphene oxide acidity and relating behavior of oxygen-containing groups in water. *Carbon*, 183, 355–361.

Monteiro Riviere, N. A., Inman, A. O., & Zhang, L. W. (2009). Limitations and relative utility of screening assays to assess engineered nanoparticle toxicity in a human cell line. *Toxicology and Applied Pharmacology*, 234(2), 222–235.

Murphy, O. P., Vashishtha, M., Palanisamy, P., Kumar, K. V. (2023). A review on the adsorption isotherms and design calculations for the optimization of adsorbent mass and contact time. *ACS Omega*, 8(20), 17407–17430.

Nair, R. R., Blake, P., Grigorenko, A. N., Novoselov, K. S., Booth, T. J., Stauber, T., Peres, N. M., & Geim, A. K. (2008). Fine structure constant defines visual transparency of graphene. *Science, 320*(5881), 1308.

Nel, A. E., Mädler, L., Velegol, D., Xia, T., Hoek, E. M., Somasundaran, P., Klaessig, F., Castranova, V., & Thompson, M. (2009). Understanding biophysicochemical interactions at the nano-bio interface. *Nature Materials*, 8(7), 543–557.

Seabra, A. B., Paula, A. J., De Lima, R., Alves, O. L., & Durán, N. (2014). Nanotoxicity of graphene and graphene oxide. *Chemical Research in Toxicology*, 27(2), 159–168.

van Meerloo, J., Kaspers, G. J., & Cloos, J. (2011). Cell sensitivity assays: The MTT assay. *Methods in Molecular Biology*, 731, 237–245.

Wang, J., Guo, X. (2020). Adsorption isotherm models: Classification, physical meaning, application and solving method. *Chemosphere*, 258, 127279.

Wei, X. Q., Hao, L. Y., Shao, X. R., Zhang, Q., Jia, X. Q., Zhang, Z. R., Lin, Y. F., & Peng, Q. (2015). Insight into the interaction of graphene oxide with serum proteins and the impact of the degree of reduction and concentration. *ACS Applied Materials & Interfaces, 7*(24), 13367–13374.

Wörle-Knirsch, J. M., Pulskamp, K., & Krug, H. F. (2006). Oops they did it again! Carbon nanotubes hoax scientists in viability assays. *Nano Letters*, 6(6), 1261–1268.

Aknowledgements

This work has been supported by the Ministry of Science, Higher Education, and Youth of Sarajevo Canton (grant No: 27-02-11-41250-2/21).

Summary/Sažetak

Velika geometrijska površina bogata kiseoničnim funkcionalnim grupama, zaslužna za interakcije sa različitim molekulama, čini grafen oksid (GO) pogodnim za primjenu u senzorima, imidžingu i terapijama, ali istovremeno komplikuje procjenu citotoksičnosti primjenom standardnih kolorimetrijskih testova. U ovom radu je ispitana adsorpcija tetrazolijum (MTT) jona, koji se koristi u kolorimetrijskim testovima, na GO. Koristeći sistem bez ćelija, adsorpciono ponašanje je opisano pomoću Frojdlihove, Lengmirove i Lengmir-Frojndlihove (Sipsove) izoterme. Zadovoljavajuće korelacije su dobijene pomoću svih modela, pri čemu je Sipsov model pokazao najbolje rezultate za nelinearnu regresiju, dok je Lengmirov model najviše odgovarao za linearnu regresiju. π–π interakcije između MTT i aromatskih prstenova GO najvjerovatnije predstavljaju glavni uzrok adsorpcije. Interakcije između GO i komponenti medija za ćelijske kulture (DMEM) i seruma (FBS) su opažene indirektno, poređenjem vrijednosti za kapacitet monosloja. Rezultati potvrđuju da interakcije između GO i MTT, odgovorne za interferencije, mogu biti kvantitativno opisane u prisustvu medija za ćelijske kulture i da je potrebno uvesti korekcije rezultata kolorimetrijskih testova. Međutim, još uvijek nije jasno da li se ove korekcije mogu jednostavno upotrijebiti u praksi. Ova studija predstavlja podlogu za procjenu isplativosti uvođenja korekcija.